Sensitivity of heavy-quark dipolar flow to its initial spatial distributions in Cu + Au collisions

Ankit Kumar Panda [*]
Key Laboratory of Quark and Lepton Physics (MOE) and Institute of Particle Physics, Central China Normal University, Wuhan 430079, China

Tribhuban Parida [†]
Faculty of Physics and Applied Computer Science, AGH University of Krakow, Aleja Mickiewicza 30, 30-059 Cracow, Poland

(Received 30 May 2026; revised 7 August 2026; accepted 28 August 2026; published 11 September 2026)

We investigate charm-quark dynamics in asymmetric Cu + Au collisions at top energies available at the BNL Relativistic Heavy Ion Collider using a Langevin approach embedded in a realistic hydrodynamic background. The intrinsic asymmetry of the colliding nuclei leads to a spatially lopsided initial energy-density profile, which generates a dipolar flow structure in the transverse plane even at midrapidity. As charm quarks propagate through this medium, they acquire a finite directed flow, v_1. We find that the p_T-integrated heavy-quark v_1 is approximately an order of magnitude larger than that of charged hadrons. In addition, the p_T-differential v_1 exhibits strong sensitivity to the initial spatial distribution of heavy quarks, highlighting the potential impact of preequilibrium modifications of the heavy-quark phase-space distribution on final-state anisotropies. Beyond geometric effects, v_1 also provides direct sensitivity to medium interactions through the temperature-dependent drag coefficient. Its pronounced dependence on this transport input indicates that precision measurements of heavy-flavor directed flow could place meaningful constraints on heavy-quark transport coefficients, thereby improving Langevin-based descriptions and predictive power for heavy-flavor observables in heavy-ion collisions.

DOI: 10.1103/nrkh-pmwk

I. INTRODUCTION

Heavy quarks serve as powerful probes of the quark-gluon plasma (QGP) [1–4] produced in high-energy heavy-ion collisions. Created predominantly in initial hard scatterings, charm and bottom quarks traverse the entire space-time evolution of the medium before hadronization [5–7]. Their large masses ensure early production and sustained interaction with the expanding plasma, making heavy-flavor observables particularly sensitive to the transport properties and dynamical evolution of the QGP [8–13]. This sensitivity is reflected in measurements of the nuclear modification factor (R_{AA}) and anisotropic flow coefficients [14–21].

Among these observables, the directed flow coefficient $v_1(y_p, p_T) = \langle \cos(\phi - \Psi) \rangle$ quantifies the first harmonic of the azimuthal particle distribution, where ϕ is the particle azimuthal angle, y_p and p_T denote rapidity and transverse momentum, and Ψ is the reference-plane angle. As an early-time observable, v_1 is sensitive to a variety of mechanisms, including the three-dimensional initial energy-density profile, event-by-event geometric asymmetries, and electromagnetic fields generated in noncentral collisions [22–26]. In particular, heavy-flavor v_1 [27–30] provides enhanced sensitivity to the early-time propagation of heavy quarks through the evolving QGP background.

In noncentral collisions, the bulk medium develops a forward-backward asymmetric tilted geometry due to unequal energy deposition in the overlap region. Heavy quarks, however, are produced in initial binary nucleon-nucleon collisions and approximately follow the binary-collision profile, leading to a spatial mismatch between the heavy-quark distribution and the tilted medium at finite rapidity. Within Langevin dynamics coupled to hydrodynamic evolution, this mismatch generates a finite heavy-quark directed flow. In this framework, heavy-flavor v_1 typically inherits the sign of the bulk flow while attaining a substantially larger magnitude [31].

Since heavy quarks are produced before local thermalization, they experience a preequilibrium stage before the onset of hydrodynamic evolution. During this interval, their spatial distribution may be modified by processes such as free streaming, diffusion, or interactions with a preequilibrium medium. The precise process of these modifications remains uncertain. Since directed flow originates from the relative spatial configuration between heavy quarks and the asymmetric medium, the final v_1 provides a sensitive probe of such early-time modifications. In this work, rather than modeling a specific preequilibrium evolution, we investigate its possible impact by varying the initial heavy-quark spatial distributions at the beginning of the hydrodynamic evolution. While preequilibrium effects on heavy-flavor observables such as R_{AA} and v_2 have been studied previously [32–36], their impact on directed flow remains largely unexplored.

Directed flow can arise from multiple sources, including tilted initial geometries [37], initial-state fluctuations [38],

[*]Contact author: ankitkumarpanda932@gmail.com
[†]Contact author: tribhu.451@gmail.com

and possible charge-dependent deflections induced by strong electromagnetic fields in noncentral collisions [24,26,39–42]. Phenomenological tilted-fireball models [37,43] typically introduce the required asymmetry through additional parameters, leading to a degree of model dependence even when constrained by charged-hadron directed flow [29,31]. By comparison, asymmetric collision systems such as Cu + Au [44–46] naturally generate an uneven transverse geometry due to the different sizes and density profiles of the colliding nuclei [47,48], providing a more constrained and physically transparent framework for studying heavy-flavor directed flow. The intrinsic dipolar deformation of the initial energy density in such systems generates a sizable rapidity-even v_1 [38,47,49–51] near midrapidity, where experimental measurements benefit from larger particle yields and improved statistical precision. The present work focuses on this geometrically driven rapidity-even component. Although event-by-event fluctuations are not included in our framework, a finite v_1 still emerges at midrapidity purely from the underlying geometric asymmetry, implying that the observed signal is dominated by the collective response to the asymmetric initial geometry. By contrast, the rapidity-odd component originates from forward-backward asymmetry in particle production, changes sign across midrapidity, and vanishes at $y_p \simeq 0$.

This paper is organized as follows. In Sec. II, we describe the heavy-quark dynamics in the hydrodynamic background, including the initial conditions, collision geometry, and medium evolution setup. Section III presents the numerical results and discusses the effects of different spatial sampling schemes on heavy-quark observables. Finally, Section IV summarizes the main findings and outlines possible directions for future investigations.

II. HEAVY-QUARK DYNAMICS IN A HYDRODYNAMIC MEDIUM

We investigate the evolution of heavy quarks, particularly charm quarks, in the hot and dense medium created in asymmetric Cu + Au collisions at top energies available at the BNL relativistic heavy ion collider (RHIC) by combining relativistic hydrodynamics with Langevin dynamics. The hydrodynamic evolution provides the spacetime profiles of the fluid velocity $u^\mu(x)$ and the temperature $T(x)$, which together define the dynamical background through which heavy quarks propagate. The medium evolution is initialized using energy density profiles obtained from a Monte Carlo Glauber model with 20 000 events, ensuring a smooth initial condition, with the hydrodynamic evolution starting at an initialization time of $\tau_0 = 0.4$ fm. In our setup, the Cu nucleus is positioned at $-b/2$ and the Au nucleus at $+b/2$ along the impact parameter axis (x axis). We emphasize that this choice of orientation is purely conventional and does not affect the physics or the conclusions presented in this work. The shear viscosity to entropy density ratio is fixed at $\eta/s = 0.08$, while the bulk viscosity ζ/s is taken to be temperature dependent [52]. The hydrodynamic evolution is continued until the local temperature reaches 145 MeV, below which hadronization is assumed to take place.

The propagation of heavy quarks through this evolving medium is described using Langevin dynamics [11,53–55], which, in the post-point realization, can be written as

$$\Delta \mathbf{r}_i = \frac{\mathbf{p}_i}{E}\Delta t,$$
$$\Delta \mathbf{p}_i = -\gamma(T)\mathbf{p}_i\Delta t + \rho_i\sqrt{2D\Delta t}, \quad (1)$$

where $\Delta \mathbf{r}_i$ and $\Delta \mathbf{p}_i$ denote the changes in the position and momentum of a heavy quark during a time step, Δt, with $i = x, y, z$. Here, $\gamma(T)$ and D represent the drag and diffusion coefficients, respectively, which characterize the interaction of heavy quarks with the medium. The drag coefficient is taken to be temperature dependent in order to reflect the evolving properties of the QGP, and we explicitly investigate the sensitivity of our results to different temperature dependencies of $\gamma(T)$. The stochastic term ρ_i is sampled independently from a Gaussian distribution at each time step and satisfies $\langle \rho_i \rangle = 0$ and $\langle \rho_i \rho_j \rangle = \delta_{ij}$. The drag and diffusion coefficients are connected through the fluctuation-dissipation theorem, and for a thermalized medium the diffusion coefficient is chosen as $D = \gamma(T)ET$, where $E = \sqrt{\mathbf{p}^2 + m^2}$ is the heavy-quark energy. This choice ensures that the heavy-quark phase-space distribution approaches the equilibrium Boltzmann-Juttner distribution in the long-time limit [56]. Since the Langevin evolution is performed in the local rest frame of the fluid, the heavy-quark phase-space coordinates are Lorentz transformed to the local fluid frame at each time step and subsequently transformed back to the laboratory frame after the momentum update.

To explore the sensitivity of heavy-quark evolution to the initial conditions, we consider three different sampling schemes for the initial phase-space distribution: (i) sampling according to the energy density profile of the medium, (ii) sampling based on the binary collision ($N_{\rm coll}$) distribution associated with the initial hard scatterings, and (iii) sampling from a uniform box-type distribution within the region $x, y \in [-2, 2]$ fm, the details of which are discussed in the next section with a pictorial depiction showing a sampling comparison in Fig. 3. The initial momentum distribution of heavy quarks is generated using the fixed order plus next-to-leading logarithm framework [57,58], which successfully reproduces the D-meson spectra measured in proton-proton collisions after fragmentation [11]. In total, 5×10^6 heavy quarks are sampled to ensure sufficient statistical precision in the analysis. To quantify the collective motion of heavy quarks, we compute the event-averaged directed flow, $v_1 = \langle p_x/p_T \rangle$. The results presented in Sec. III illustrate the effects of different initial sampling schemes, impact parameters, and temperature dependencies of the drag coefficient on the heavy-quark distributions and directed flow. In Fig. 1, we show the initial energy density profile at $b = 6$ fm, which serves as the input for the subsequent hydrodynamic evolution performed using the music hydrodynamic framework [59–61]. Although additional calculations are carried out for other impact parameters to study the influence of varying initial geometries, they are not shown here. Comparisons between different sampling prescriptions, momentum spectra, and drag-coefficient parametrizations provide insight into the interplay between

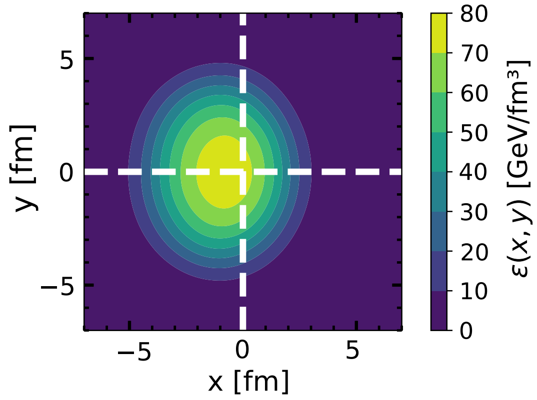

FIG. 1. Initial energy density profile for a Cu + Au collision at $b = 6$ fm, with Cu at $-b/2$ and Au at $b/2$, used as input for the music hydrodynamic evolution at $\sqrt{s_{NN}} = 200$ GeV.

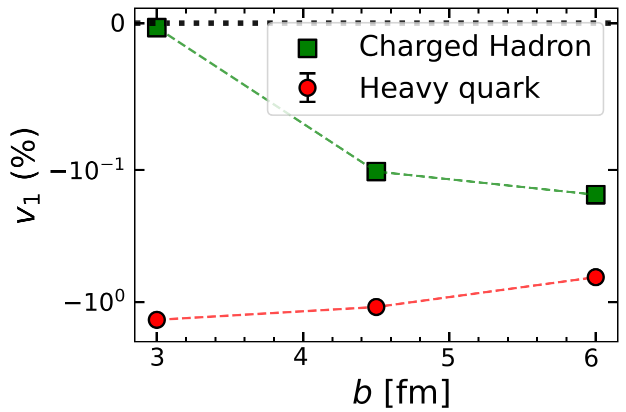

FIG. 2. Comparison of integrated v_1 versus impact parameter for light ($p_T \in [0, 3]$ GeV) and heavy ($p_T \in [0, 10]$ GeV) quarks, calculated with $\gamma(T) = 0.6\,T$ using $N_{\rm coll}$ sampling.

the initial geometry, medium evolution, and drag-diffusion dynamics in shaping heavy-quark collectivity.

III. RESULTS AND DISCUSSIONS

The initial energy density profile exhibits a pronounced asymmetry in the transverse plane, reflecting the intrinsic size difference between the colliding nuclei. In the collision geometry, the Cu nucleus is shifted by $-b/2$ and the Au nucleus by $+b/2$ along the impact parameter direction (x axis), as discussed earlier. Due to its smaller transverse thickness, the Cu nucleus deposits less energy compared to the thicker Au nucleus, resulting in a spatially lopsided energy density distribution, as illustrated in Fig. 1. This asymmetry is most prominent along the impact parameter direction: the energy density varies significantly along the x axis, while remaining approximately symmetric along the y axis. As a consequence, the pressure gradients generated during the subsequent hydrodynamic evolution are themselves asymmetric along the positive and negative x directions. Such an initial asymmetry drives a preferential collective expansion from the negative toward the positive x direction, leading to an imbalance in the final-state transverse momentum component p_x. This momentum anisotropy gives rise to a nonzero directed flow (v_1) of charged hadrons. The p_T-integrated charged-hadron v_1 for different impact parameters is shown as square markers in Fig. 2. As collisions become more peripheral, the geometric asymmetry of the overlap region becomes more pronounced, amplifying the asymmetry in the pressure gradients and, consequently, the directed flow signal. Accordingly, the magnitude of charged-hadron v_1 increases from central to peripheral collisions, as illustrated in Fig. 2.

It should be noted that the directed flow presented here is computed with respect to the reaction plane (see Sec. I). In our simulations, the reaction plane angle is set to 0 by aligning the impact parameter vector along the x axis. Experimentally, the reaction plane angle—defined as the angle between the reaction plane and the laboratory x axis—is not directly measurable, but can be inferred from the spectator plane reconstructed using spectator nucleons [62].

To study heavy-quark dynamics in such an asymmetric medium, we initialize their production points according to the binary collision ($N_{\rm coll}$) distribution and evolve them using Langevin dynamics on the hydrodynamic background. The schematic sampling using the real data is shown in Fig. 3, where we display the energy density distribution along the x axis at $y = 0$, together with the corresponding binary collision distribution projected onto the same axis. A clear difference emerges when comparing the spatial distributions of the medium energy density, which drives the flow of charged hadrons, with the heavy-quark production points obtained from $N_{\rm coll}$. This offset between the mean positions of the medium and heavy-quark distributions plays a decisive role in shaping the final directed flow.

Heavy quarks originating from different locations within the medium experience unequal interactions, undergoing asymmetric drag along the positive and negative x directions, which gives rise to a finite heavy-quark v_1. The resulting p_T-integrated charm-quark v_1, calculated within our framework, is shown alongside that of charged hadrons in Fig. 2. When

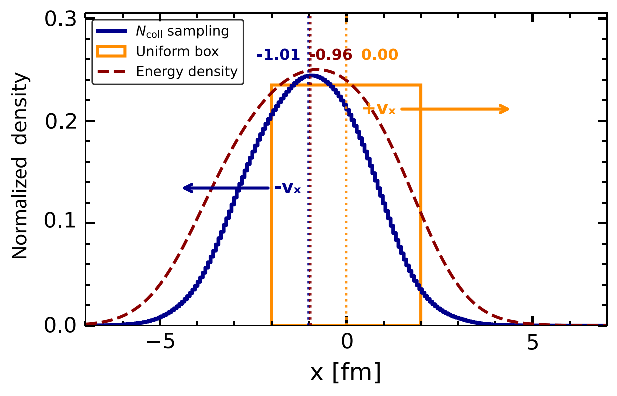

FIG. 3. Initial heavy-quark distributions along the impact-parameter (x) axis at $y = 0$ for a Cu + Au collision with $b = 6$ fm at $\sqrt{s_{NN}} = 200$ GeV. Shown are three distributions: two from the Monte Carlo Glauber model and one uniform (box-type) distribution, with their means -1.01, -0.96, and 0.00 for $N_{\rm coll}$, energy density, and uniform box samplings, respectively.

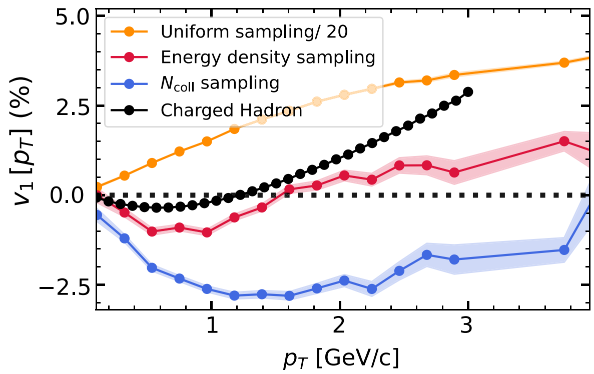

FIG. 4. Comparison of v_1 for different heavy-quark sampling methods at $b = 6$ fm, $y_p \in [-1,1]$ with $\gamma(T) = 1.2\,T$. Shaded bands indicate statistical uncertainties.

compared to the light-flavor-dominated charged hadrons, the heavy-quark v_1 is roughly an order of magnitude larger while retaining the same sign across impact parameters up to $b = 6$ fm. This behavior can be traced back to the relative spatial distributions illustrated in Fig. 3: the heavy-quark production profile is shifted to the left of the energy density distribution (mean -1.01 versus -0.96 for the energy density), indicating that a larger fraction of heavy quarks initially resides on one side of the medium and consequently experiences asymmetric drag during their evolution. This effect is quantified through the mean values indicated in Fig. 3. Furthermore, the difference in their mean in these distributions gradually increases toward more central collisions, amplifying the difference in the most-central events.

Motivated by the early production of heavy quarks and the observed sensitivity of their directed flow (v_1) to the relative spatial distributions of heavy quarks and the medium energy density, we investigate how different initialization schemes influence final-state heavy-flavor observables. For this we consider three initialization procedures. In the first scenario, heavy quarks are sampled according to the binary collision (N_{coll}) distribution, representing the conventional assumption based on production through initial hard scatterings. In the second scenario, heavy quarks are initialized following the energy density profile of the medium. Finally, in the third scenario, heavy quarks are uniformly sampled within a box centered at $(x, y) = (0, 0)$ in the transverse plane. These three distributions are illustrated in Fig. 3, providing a clear comparison of the relative positions of heavy quarks with respect to the medium and offering intuition for the expected sign and magnitude of the resulting directed flow. The corresponding heavy-quark $v_1(p_T)$ for each initialization scheme is presented in Fig. 4 for collisions with impact parameter $b = 6$ fm and a temperature-dependent drag coefficient of $\gamma(T) = 1.2\,T$. For reference, the $v_1(p_T)$ of charged hadrons obtained from the music hydrodynamic simulation is also shown.

The results indicate that the heavy-quark directed flow exhibits a strong dependence on the initialization procedure, displaying qualitatively different behaviors across the scenarios. When heavy quarks are sampled uniformly in the box, most are initially located to the right of the energy density maximum, resulting in a strongly positive v_1. In contrast, N_{coll} sampling positions the majority of heavy quarks to the left of the maximum, yielding a negative v_1. Sampling along the energy density profile places heavy quarks near the medium peak, producing a v_1 that transitions from negative at low p_T to positive at intermediate p_T, a similar trend shown by the light charged hadron's v_1.

These findings demonstrate that both the sign and the magnitude of v_1, as well as its transverse momentum dependence, are strongly influenced by the initial spatial distribution of heavy quarks. Measuring the directed flow (v_1) of heavy quarks in asymmetric collisions can provide valuable information about their spatial distribution at the onset of the hydrodynamic evolution. Although heavy quarks are produced at very early times through hard scatterings, their distribution at $\tau_0 = 0.4$ fm/c may differ from the original production profile due to possible preequilibrium dynamics. By studying different initializations at the hydrodynamic starting time, future measurements of heavy-flavor v_1 can help constrain whether such early-time modifications are significant.

The directed flow of heavy quarks is also influenced by their interactions with the medium, which are described by the Langevin drag coefficient. By exploring different parametrizations of the drag, we can investigate how v_1 reflects both the initial geometry and the heavy-quark transport properties. In this study, the drag coefficient is defined as $\gamma(T) = \gamma_0 T(\frac{T}{m})^x$, where γ_0 controls the overall interaction strength, for which we consider values of 0.6 and 1.2 in the present study, while x governs the additional temperature dependence and is taken to be either 0 or 1/2. In addition to these temperature-dependent parametrizations, we also explore a phenomenological momentum-dependent form of the drag coefficient, $\gamma(p, T) = \gamma_0 T(\frac{m}{E})^{0.5}$, to examine the possible impact of momentum dependence on the heavy-quark directed flow. This parametrization is not intended to represent a microscopic calculation of the transport coefficient, but rather serves as a simple phenomenological extension motivated by the expected qualitative behavior of momentum-dependent energy loss. In this form, the drag coefficient reduces to the purely temperature-dependent expression in the low-momentum limit ($E \to m$), while it gradually decreases with increasing heavy-quark momentum, reflecting the weaker interaction strength expected for highly energetic quarks. Using these variations, we calculate v_1 while keeping the initial heavy-quark distribution fixed to N_{coll} sampling. The resulting heavy-flavor v_1 is shown in Fig. 5. While the overall trend of v_1 remains similar, its magnitude increases with stronger drag, highlighting the sensitivity of heavy-quark directed flow to the transport properties of the medium.

The drag coefficient affects not only heavy-quark directed flow but also other key observables, such as the nuclear modification factor R_{AA} and the elliptic flow v_2 [31]. Among these, the directed flow v_1 offers an independent and complementary probe of heavy-quark transport. Unlike R_{AA} and v_2, which mainly reflect energy loss and momentum anisotropy, v_1 is directly sensitive to the relative spatial configuration of heavy-quark production and the asymmetric medium. Its ability to change sign makes it particularly responsive to both the initial geometry and the transport dynamics. A combined analysis of

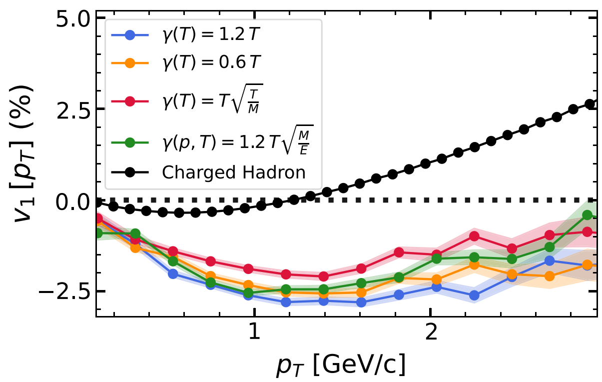

FIG. 5. Comparison of v_1 for heavy quarks and light charged hadrons at $b = 6$ fm, $y_p \in [-1,1]$ showing sensitivity to the temperature and momentum dependence of the drag coefficient. Heavy quarks are sampled via N_{coll}; shaded bands indicate statistical uncertainties.

v_1, R_{AA}, and v_2 can therefore reduce uncertainties in the temperature dependence of heavy-quark transport and improve the overall modeling of heavy-quark evolution in the medium.

We emphasize that the present results are not directly for D mesons, as hadronization via fragmentation or coalescence, as well as subsequent hadronic rescattering and freeze-out effects, are not included in this study; while these effects may modify the results quantitatively, the qualitative features and underlying trends are expected to remain unchanged. This expectation has been checked by applying the standard Peterson fragmentation prescription to the final-state charm quarks, which confirms that the qualitative features of the directed flow remain preserved after fragmentation.

IV. CONCLUSION

We have investigated the directed flow (v_1) of heavy quarks in asymmetric Cu + Au collisions at $\sqrt{s_{NN}} = 200$ GeV using hydrodynamics coupled with Langevin dynamics. Our results demonstrate that heavy-quark v_1 is highly sensitive to their initial spatial distribution relative to the medium energy density. Depending on the initialization scheme—binary collision (N_{coll}), energy-density profile, or uniform box—the sign, magnitude, and p_T dependence of v_1 can vary substantially, underscoring the critical role of early-time heavy-quark positioning in shaping final-state observables. The magnitude of v_1 increases with stronger drag, reflecting its sensitivity to medium transport properties. Compared to the p_T-integrated v_1 of light-flavor hadrons, the heavy-quark signal is roughly an order of magnitude larger across the centralities studied (up to $b = 6$ fm), arising from the asymmetric drag experienced in the lopsided energy density profile. In conjunction with other observables such as elliptic flow (v_2) and the nuclear modification factor (R_{AA}), v_1 offers a complementary probe of heavy-quark interactions in the quark-gluon plasma.

These findings suggest that similar effects may arise in other asymmetric systems, such as Pb + O, where geometric asymmetry could generate analogous heavy-flavor v_1 signals. Additionally, asymmetric collisions produce highly nonuniform electromagnetic fields. Incorporating electromagnetic effects in future studies could illuminate the interplay between medium-induced and electromagnetic contributions to heavy-quark directed flow, complementing prior investigations that focused mainly on symmetric collisions [27,30,63].

In summary, heavy-quark v_1 in asymmetric collisions emerges as a sensitive probe of both the initial geometry and the transport properties of the medium. Experimental measurements of heavy-flavor directed flow can directly constrain the early-time spatial distribution of heavy quarks and their interactions with the quark-gluon plasma, offering new insights into heavy-flavor dynamics in high-energy nuclear collisions.

ACKNOWLEDGMENTS

A.K.P. is supported by Central China Normal University and by the NSFC under Grant No. 12435009. T.P. acknowledges support from the AGH University of Krakow and the Polish National Science Centre under Grant No. 2023/51/B/ST2/01625.

DATA AVAILABILITY

There are no publicly available research data or software supporting this manuscript. Requests for further information or data should be sent to the authors.

[1] H. Song, S. A. Bass, U. Heinz, T. Hirano, and C. Shen, 200 *A* GeV Au + Au collisions serve a nearly perfect quark-gluon liquid, Phys. Rev. Lett. **106**, 192301 (2011); **109**, 139904(E) (2012).

[2] W. Busza, K. Rajagopal, and W. van der Schee, Heavy ion collisions: The big picture and the big questions, Annu. Rev. Nucl. Part. Sci. **68**, 339 (2018).

[3] P. F. Kolb, J. Sollfrank, and U. W. Heinz, Anisotropic transverse flow and the quark-hadron phase transition, Phys. Rev. C **62**, 054909 (2000).

[4] U. Heinz and R. Snellings, Collective flow and viscosity in relativistic heavy-ion collisions, Annu. Rev. Nucl. Part. Sci. **63**, 123 (2013).

[5] R. Rapp, D. Blaschke, and P. Crochet, Charmonium and bottomonium in heavy-ion collisions, Prog. Part. Nucl. Phys. **65**, 209 (2010).

[6] M. He, R. J. Fries, and R. Rapp, Heavy flavor at the large hadron collider in a strong coupling approach, Phys. Lett. B **735**, 445 (2014).

[7] A. Andronic, P. Braun-Munzinger, M. K. Köhler, A. Mazeliauskas, K. Redlich, J. Stachel, and V. Vislavicius, The multiple-charm hierarchy in the statistical hadronization model, J. High Energy Phys. 07 (2021) 035.

[8] R. Rapp *et al.*, Extraction of heavy-flavor transport coefficients in QCD matter, Nucl. Phys. A **979**, 21 (2018).

[9] S. Cao, G.-Y. Qin, and S. A. Bass, Heavy-quark dynamics and hadronization in ultrarelativistic heavy-ion collisions: Collisional versus radiative energy loss, Phys. Rev. C **88**, 044907 (2013).

[10] S. Cao *et al.*, Toward the determination of heavy-quark transport coefficients in quark-gluon plasma, Phys. Rev. C **99**, 054907 (2019).

[11] F. Scardina, S. K. Das, V. Minissale, S. Plumari, and V. Greco, Estimating the charm quark diffusion coefficient and thermalization time from D meson spectra at energies available at the BNL relativistic heavy ion collider and the CERN large hadron collider, Phys. Rev. C **96**, 044905 (2017).

[12] S. K. Das, J.-e Alam, and P. Mohanty, Probing quark gluon plasma properties by heavy flavors, Phys. Rev. C **80**, 054916 (2009).

[13] S. K. Das, J. M. Torres-Rincon, and R. Rapp, Charm and bottom hadrons in hot hadronic matter, Phys. Rep. **1129–1131**, 1 (2025).

[14] G. D. Moore and D. Teaney, How much do heavy quarks thermalize in a heavy ion collision? Phys. Rev. C **71**, 064904 (2005).

[15] S. L. Olsen, T. Skwarnicki, and D. Zieminska, Nonstandard heavy mesons and baryons: Experimental evidence, Rev. Mod. Phys. **90**, 015003 (2018).

[16] J. W. Harris and B. Müller, "QGP signatures" revisited, Eur. Phys. J. C **84**, 247 (2024).

[17] J. Adam *et al.* (STAR Collaboration), Centrality and transverse momentum dependence of D^0-meson production at mid-rapidity in Au + Au collisions at $\sqrt{s_{NN}} = 200$ GeV, Phys. Rev. C **99**, 034908 (2019).

[18] S. K. Das, F. Scardina, S. Plumari, and V. Greco, Toward a solution to the R_{AA} and v_2 puzzle for heavy quarks, Phys. Lett. B **747**, 260 (2015).

[19] W. M. Alberico, A. Beraudo, A. De Pace, A. Molinari, M. Monteno, M. Nardi, F. Prino, and M. Sitta, Heavy flavors in *AA* collisions: Production, transport and final spectra, Eur. Phys. J. C **73**, 2481 (2013).

[20] S. Cao, G.-Y. Qin, and S. A. Bass, Energy loss, hadronization, and hadronic interactions of heavy flavors in relativistic heavy-ion collisions, Phys. Rev. C **92**, 024907 (2015).

[21] M. He, R. J. Fries, and R. Rapp, Heavy-quark diffusion and hadronization in quark-gluon plasma, Phys. Rev. C **86**, 014903 (2012).

[22] C. Alt *et al.* (NA49 Collaboration), Directed and elliptic flow of charged pions and protons in Pb + Pb collisions at 40*A* and 158*A* GeV, Phys. Rev. C **68**, 034903 (2003).

[23] C. Shen and S. Alzhrani, Collision-geometry-based 3D initial condition for relativistic heavy-ion collisions, Phys. Rev. C **102**, 014909 (2020).

[24] U. Gürsoy, D. Kharzeev, and K. Rajagopal, Magnetohydrodynamics, charged currents, and directed flow in heavy ion collisions, Phys. Rev. C **89**, 054905 (2014).

[25] L. Adamczyk *et al.* (STAR Collaboration), Beam-energy dependence of the directed flow of protons, antiprotons, and pions in Au + Au collisions, Phys. Rev. Lett. **112**, 162301 (2014).

[26] A. K. Panda, R. Gangadharan, and V. Roy, Investigating the role of electric fields on flow harmonics in heavy-ion collisions, J. Phys. G: Nucl. Part. Phys. **50**, 075102 (2023).

[27] S. K. Das, S. Plumari, S. Chatterjee, J. Alam, F. Scardina, and V. Greco, Directed flow of charm quarks as a witness of the initial strong magnetic field in ultra-relativistic heavy ion collisions, Phys. Lett. B **768**, 260 (2017).

[28] Y. Sun, S. Plumari, and S. K. Das, Exploring the effects of electromagnetic fields and tilted bulk distribution on directed flow of D mesons in small systems, Phys. Lett. B **843**, 138043 (2023).

[29] S. Chatterjee and P. Bozek, Interplay of drag by hot matter and electromagnetic force on the directed flow of heavy quarks, Phys. Lett. B **798**, 134955 (2019).

[30] A. K. Panda, Pooja, M. L. Sambataro, S. Plumari, and S. K. Das, Directed flow of D and B mesons in an electrically and chirally conductive QGP at LHC energies, Phys. Lett. B **880** 140794 (2026),.

[31] S. Chatterjee and P. Bożek, Large directed flow of open charm mesons probes the three-dimensional distribution of matter in heavy-ion collisions, Phys. Rev. Lett. **120**, 192301 (2018).

[32] S. K. Das, M. Ruggieri, F. Scardina, S. Plumari, and V. Greco, Effect of pre-equilibrium phase on R_{AA} and v_2 of heavy quarks in heavy ion collisions, J. Phys. G: Nucl. Part. Phys. **44**, 095102 (2017).

[33] M. Singh, M. Kurian, B. Schenke, S. Jeon, and C. Gale, Charm quark evolution in the early stages of heavy-ion collisions, Phys. Rev. C **113**, 024904 (2026).

[34] S. K. Das, M. Ruggieri, S. Mazumder, V. Greco, and J. Alam, Heavy quark diffusion in the pre-equilibrium stage of heavy ion collisions, J. Phys. G: Nucl. Part. Phys. **42**, 095108 (2015).

[35] Y. Sun, G. Coci, S. K. Das, S. Plumari, M. Ruggieri, and V. Greco, Impact of glasma on heavy quark observables in nucleus-nucleus collisions at LHC, Phys. Lett. B **798**, 134933 (2019).

[36] M. Ruggieri, F. Scardina, S. Plumari, and V. Greco, Elliptic flow from non-equilibrium initial condition with a saturation scale, Phys. Lett. B **727**, 177 (2013).

[37] P. Bożek and I. Wyskiel, Directed flow in ultrarelativistic heavy-ion collisions, Phys. Rev. C **81**, 054902 (2010).

[38] M. Luzum and J.-Y. Ollitrault, Directed flow at midrapidity in heavy-ion collisions, Phys. Rev. Lett. **106**, 102301 (2011).

[39] L. Adamczyk *et al.* (STAR Collaboration), Charge-dependent directed flow in Cu + Au collisions at $\sqrt{s_{NN}} = 200$ GeV, Phys. Rev. Lett. **118**, 012301 (2017).

[40] M. I. Abdulhamid *et al.* (STAR Collaboration), Observation of the electromagnetic field effect via charge-dependent directed flow in heavy-ion collisions at the relativistic heavy ion collider, Phys. Rev. X **14**, 011028 (2024).

[41] J. Jia, Event-shape fluctuations and flow correlations in ultra-relativistic heavy-ion collisions, J. Phys. G: Nucl. Part. Phys. **41**, 124003 (2014).

[42] J. Y. Zhang, Y. J. Song, L. Ma, W. H. Ma, and H. Z. Huang, Effect of initial geometry fluctuations on the heavy flavor flow using a multiphase transport model, Phys. Rev. C **112**, 044901 (2025).

[43] T. Parida and S. Chatterjee, Splitting of elliptic flow in a tilted fireball, Phys. Rev. C **106**, 044907 (2022).

[44] V. Voronyuk, V. D. Toneev, S. A. Voloshin, and W. Cassing, Charge-dependent directed flow in asymmetric nuclear collisions, Phys. Rev. C **90**, 064903 (2014).

[45] A. Adare *et al.* (PHENIX Collaboration), Pseudorapidity dependence of particle production and elliptic flow in asymmetric nuclear collisions of p + Al, p + Au, d + Au, and ^{3}He + Au at $\sqrt{s_{NN}} = 200$ GeV, Phys. Rev. Lett. **121**, 222301 (2018).

[46] K. Nakamura, T. Miyoshi, C. Nonaka, and H. R. Takahashi, Directed flow in relativistic resistive magneto-hydrodynamic expansion for symmetric and asymmetric collision systems, Phys. Rev. C **107**, 014901 (2023).

[47] P. Bożek, Event-by-event viscous hydrodynamics for Cu–Au collisions at $\sqrt{s_{NN}} = 200$ GeV, Phys. Lett. B **717**, 287 (2012).

[48] A. Adare *et al.* (PHENIX Collaboration), Measurements of directed, elliptic, and triangular flow in Cu + Au collisions at $\sqrt{s_{NN}} = 200$ GeV, Phys. Rev. C **94**, 054910 (2016).

[49] D. Teaney and L. Yan, Triangularity and dipole asymmetry in relativistic heavy ion collisions, Phys. Rev. C **83**, 064904 (2011).

[50] F. G. Gardim, F. Grassi, Y. Hama, M. Luzum, and J.-Y. Ollitrault, Directed flow at midrapidity in event-by-event hydrodynamics, Phys. Rev. C **83**, 064901 (2011).

[51] K. Shafi and S. Chatterjee, Probing nuclear geometry through multi-particle azimuthal correlations and rapidity-even dipolar flow in $^{16}O + ^{16}O$ collisions, Eur. Phys. J. C **86**, 93 (2026).

[52] J. S. Moreland, J. E. Bernhard, and S. A. Bass, Bayesian calibration of a hybrid nuclear collision model using *p*-Pb and Pb-Pb data at energies available at the CERN large hadron collider, Phys. Rev. C **101** 024911 (2020).

[53] M. He, H. van Hees, and R. Rapp, Heavy-quark diffusion in the quark–gluon plasma, Prog. Part. Nucl. Phys. **130**, 104020 (2023).

[54] H. van Hees, V. Greco, and R. Rapp, Heavy-quark probes of the quark-gluon plasma and interpretation of recent data taken at the BNL relativistic heavy ion collider, Phys. Rev. C **73**, 034913 (2006).

[55] S. Cao and S. A. Bass, Thermalization of charm quarks in infinite and finite quark-gluon plasma matter, Phys. Rev. C **84**, 064902 (2011).

[56] M. He, H. van Hees, P. B. Gossiaux, R. J. Fries, and R. Rapp, Relativistic Langevin dynamics in expanding media, Phys. Rev. E **88**, 032138 (2013).

[57] M. Cacciari, P. Nason, and R. Vogt, QCD predictions for charm and bottom quark production at RHIC, Phys. Rev. Lett. **95**, 122001 (2005).

[58] M. Cacciari, S. Frixione, N. Houdeau, M. L. Mangano, P. Nason, and G. Ridolfi, Theoretical predictions for charm and bottom production at the LHC, J. High Energy Phys. 10 (2012) 137.

[59] B. Schenke, S. Jeon, and C. Gale, (3+1)D hydrodynamic simulation of relativistic heavy-ion collisions, Phys. Rev. C **82**, 014903 (2010).

[60] B. Schenke, S. Jeon, and C. Gale, Elliptic and triangular flow in event-by-event $D = 3 + 1$ viscous hydrodynamics, Phys. Rev. Lett. **106**, 042301 (2011).

[61] J.-F. Paquet, C. Shen, G. S. Denicol, M. Luzum, B. Schenke, S. Jeon, and C. Gale, Production of photons in relativistic heavy-ion collisions, Phys. Rev. C **93**, 044906 (2016).

[62] L. Adamczyk *et al.* (STAR Collaboration), Directed flow of identified particles in Au + Au collisions at $\sqrt{S_{NN}} = 200$ GeV at RHIC, Phys. Rev. Lett. **108**, 202301 (2012).

[63] Z.-F. Jiang, S. Cao, W.-J. Xing, X.-Y. Wu, C. B. Yang, and B.-W. Zhang, Probing the initial longitudinal density profile and electromagnetic field in ultrarelativistic heavy-ion collisions with heavy quarks, Phys. Rev. C **105**, 054907 (2022).